

Twinkling pulsar wind nebulae in the synchrotron cut-off regime and the gamma-ray flares in the Crab Nebula

A.M.Bykov^{1*}, G.G.Pavlov^{2,3}, A.V.Artemyev⁴, Yu.A.Uvarov^{1,3}

¹*Ioffe Institute for Physics and Technology, 194021 St.Petersburg, Russia*

²*525 Davey Laboratory, Pennsylvania State University, University Park, PA 16802*

³*State Politechnical University, St. Petersburg, Russia*

⁴*Space Research Institute, Russian Academy of Sciences, Moscow, Russia*

8 September 2021

ABSTRACT

Synchrotron radiation of ultra-relativistic particles accelerated in a pulsar wind nebula may dominate its spectrum up to γ -ray energies. Because of the short cooling time of the γ -ray emitting e^\pm , the γ -ray emission zone is in the immediate vicinity of the acceleration site. The particle acceleration likely occurs at the termination shock of the relativistic striped wind, where multiple forced magnetic field reconnections provide strong magnetic fluctuations facilitating Fermi acceleration processes. The acceleration mechanisms imply the presence of stochastic magnetic fields in the particle acceleration region, which cause stochastic variability of the synchrotron emission. This variability is particularly strong in the steep γ -ray tail of the spectrum, where modest fluctuations of the magnetic field lead to strong flares of spectral flux. In particular, stochastic variations of magnetic field, which may lead to quasi-cyclic γ -ray flares, can be produced by the relativistic cyclotron ion instability at the termination shock. Our model calculations of the spectral and temporal evolution of synchrotron emission in the spectral cut-off regime demonstrate that the intermittent magnetic field concentrations dominate the γ -ray emission from highest energy electrons and provide fast, strong variability even for a quasi-steady distribution of radiating particles. The simulated light curves and spectra can explain the very strong γ -ray flares observed in the Crab nebula and the lack of strong variations at other wavelengths. The model predicts high polarization in the flare phase, which can be tested with future polarimetry observations.

Key words: shock waves — turbulence— ISM: supernova remnants—gamma-rays—supernovae: individual (Crab nebula)

1 INTRODUCTION

Strong flares of a few days duration have been discovered recently by the *AGILE* and *Fermi* γ -ray observatories in the Crab nebula at energies above 100 MeV (see e.g. Tavani et al. 2011; Abdo, et al. 2011; Vittorini et al 2011, and references therein). The most striking features of the flares are the extreme amplitude of the photon flux changes, especially at energies above the exponential cut-off energy of the quiescent spectrum, and the fast hour-timescale variability. While the exponential cut-off energy E_c of a typical quiescent γ -ray spectrum is ~ 100 MeV, the cut-off energy of > 500 MeV was found in the April 2011 flare spectrum. This value of E_c exceeds the energy $\tilde{E}_c \sim m_e c^2 / \alpha \sim 100$ MeV (where $\alpha = e^2 / \hbar c$ is the fine-structure constant), con-

sidered to be the maximal cut-off energy in the synchrotron models of γ -ray emission from the Crab and other pulsar wind nebulae (PWNe) (de Jager et al. 1996; Uzdensky et al. 2011; Striani et al. 2011). The value \tilde{E}_c is the synchrotron photon energy emitted by an electron whose energy is such that the synchrotron cooling time is equal to the characteristic gyration time ω_g^{-1} (see e.g. Guilbert et al. 1983; de Jager et al. 1996; Atoyan & Aharonian 1996). The particle gyration time is considered to be the fastest acceleration time in a plasma system with frozen-in magnetic field of the r.m.s. amplitude $\langle B^2 \rangle^{1/2}$ that exceeds the electric field magnitude. The value of \tilde{E}_c corresponds to the electron Lorentz factor γ_m that can be found from the equation $\dot{\mathcal{E}}_{syn}(\gamma_m) = \dot{\mathcal{E}}_{acc}(\gamma_m)$. Both the synchrotron loss rate $\dot{\mathcal{E}}_{syn}(\gamma)$ and the electron acceleration rate $\dot{\mathcal{E}}_{acc}(\gamma)$ depend on the moments (often just $\langle B^2 \rangle$) of the stochastic magnetic field.

* E-mail: byk@astro.ioffe.ru

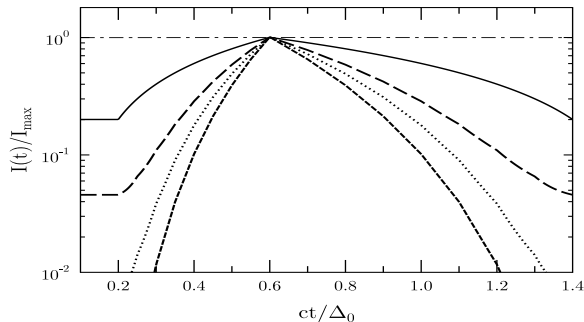


Figure 1. Light curves of synchrotron emission at 5 keV (dot-dash line), 500 MeV (dashed line), 1 GeV (dotted line) and 2 GeV (short-dash line) as a response to an imposed fluctuation with magnetic field $B(t)$ (solid line) simulated in Model I. The light curves are normalized to maximal intensity. The background magnetic field in the emission region was modeled as a stochastic gaussian field of $\langle B^2(0) \rangle^{1/2} = 0.2$ mG. The imposed fluctuation $B(t)$ (solid line) is localized in a stripe of a $0.01\Delta_0$ thickness ($\gg r_f$). The maximum of $B(t) = 1$ mG is at $ct/\Delta_0 = 0.6$. The spatial scale $\Delta_0 \approx 2 \times 10^{16}$ cm for the photon energy $E \approx 1$ GeV provides the photon variability timescale of about 10^5 s in the GeV regime.

In this work we consider the case when the formation length, $r_f = m_e c^2 / e \langle B^2 \rangle^{1/2}$, of incoherent synchrotron radiation is much smaller than the typical synchrotron cooling and acceleration lengths, while the typical wavelength λ of the fluctuating magnetic field is larger than r_f . In this case $\dot{\mathcal{E}}_{syn}(\gamma_m)$, $\dot{\mathcal{E}}_{acc}(\gamma_m)$, and E_c are determined by the same r.m.s. value of the fluctuating magnetic field, and the bulk of the relativistic electron distribution may vary on scales that are much larger than the gyration radius $r_g = \gamma r_f$. Since the synchrotron emissivity of a power-law electron distribution with spectral index p is proportional to $B^{(p+1)/2}$, the local emissivity sharply grows with B for large p values. This means that the synchrotron radiation in the cut-off regime (which corresponds to large effective p values) is governed by high statistical moments of the stochastic magnetic field distribution, and it is intermittent. The intermittency effect implies that rare strong peaks of the magnetic field distribution dominate the synchrotron emission (Bykov et al. 2008, 2009). It is particularly important in the synchrotron cut-off regime, when the typical size of the distribution of radiating electrons (the synchrotron cooling length) can be comparable with the correlation length of strong magnetic field fluctuations. For instance, this is expected to be the case in supernova shells, where magnetic fluctuations are produced by instabilities of anisotropic distributions at the maximal energy of particles accelerated in the source (see, e.g., Bykov et al. 2011, and references therein).

Since the source emission in the cut-off regime is domi-

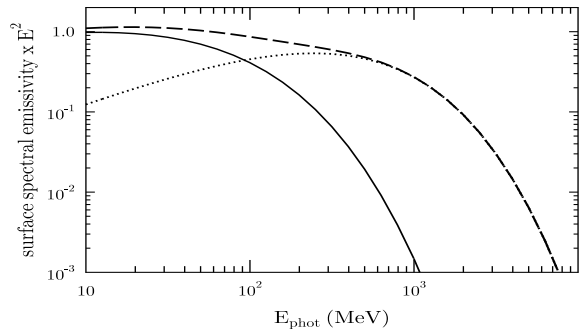


Figure 2. Normalized spectra of synchrotron radiation at two different time moments $ct/\Delta_0 = 0.2$ (solid line) and 0.6 (dashed line), which model the quiescent and flare spectra, respectively (see Fig. 1). The dotted curve shows the contribution of the variable magnetic field. The power emitted in the GeV flare is about 2×10^{36} erg s $^{-1}$, for the Crab parameters.

nated by just a single (or a few strongest) concentration(s) of the stochastic magnetic field, the light curve of the source in this regime reflects the lifetime of the magnetic concentrations rather than the electron acceleration/losses timescales. Fast temporal variations will appear even for a quasi-steady electron distribution. The light curve and the spectral behaviour in the synchrotron cut-off regime are determined by statistical characteristics of the magnetic field, which can be described by the probability distribution function (PDF) of magnetic fluctuations, $P(B)$.

It is worthwhile to note that intermittent magnetic fields can be found in quite different circumstances. For instance, non-Gaussian distributions of fluctuations, exhibiting gradual tails at large field amplitudes, have been found in the Earth magnetotail after the current disruption associated with magnetospheric substorms observed by *Geotail* and *Cluster* satellites. The energy injection during the substorms feeds an energy cascade to small-scale fluctuations with the corresponding increase of intermittency (see, e.g., Zimbardo et al. 2010, for a recent review of magnetospheric observations).

In this Letter we show that the model of synchrotron emission in fluctuating magnetic fields, with account for the intermittency in the spectral cut-off regime, can explain the nature of the γ -ray flares observed in the Crab. We demonstrate the effect of intermittency on the GeV regime emission using two models. In first model, we simulate the spectra of accelerated electrons and positrons in a simple kinetic model of diffusive Fermi acceleration in the termination shock of striped wind with account for synchrotron losses. Then we construct the GeV regime flare light curve and spectra by integrating the synchrotron emissivity of spatially inhomogeneous particle distribution in the shock downstream with imposed magnetic field variation. Second model demonstrates the effect of the magnetic field PDF shape on the syn-

chrotron photon spectra in the cut-off regime. The emission is produced by Fermi-accelerated pairs in the spectral cut-off regime, in which the acceleration is balanced by synchrotron losses.

2 MODELING

The synchrotron origin of the observed gamma-ray flares assumes the presence of pairs accelerated to PeV energies. The thickness of the γ -radiating region depends on the cooling rate in the magnetic field: $\Delta \sim \tau_{\text{syn}} c \sim 1.5 \times 10^{15} \cdot B_{\text{mG}}^{-3/2} \cdot E_{\text{GeV}}^{-1/2}$ cm, where B_{mG} is the r.m.s. magnetic field in mG, and E_{GeV} is the photon energy in GeV. The size of the γ -ray emitting region is very small compared to the size of the nebula. The thickness of the layer Δ is estimated using the standard electron synchrotron cooling time (e.g. Rybicki & Lightman 1979) of the electron radiating photons at the peak of the power spectrum of synchrotron emission. The particle acceleration mechanism in PWNe is not fully understood yet, although some basic features and constraints have been established (see, e.g., Kennel & Coroniti 1984; Arons 2008, 2011; Keshet et al. 2009; Kirk et al. 2009; Lemoine & Pelletier 2010; Sironi & Spitkovsky 2011; Bykov & Treumann 2011; Uzdensky et al. 2011).

Recent models of particle acceleration in PWNe consider a relativistic wind in the equatorial plane with toroidal stripes of opposite magnetic field polarity, separated by current sheets. Sironi & Spitkovsky (2011) modeled particle acceleration and magnetic field dissipation at the termination shock of a relativistic striped wind using 2D and 3D particle-in-cell (PIC) simulations. They found a complex structure of the flow in the vicinity of the termination shock. In that model, the shock-driven reconnection in the downstream transfers the magnetic energy of alternating fields of the striped wind to accelerated relativistic pairs. The energy spectra of electrons accelerated in the reconnection region take the form of power laws, $N(\gamma) \propto \gamma^{-p}$, with spectral indices $p \sim 1.5$ that match the radio-optical observations of the Crab nebula (e.g. Bietenholz et al. 1997; Hester 2008; Arendt et al. 2011). The accelerated particles can escape ahead of the shock and generate magnetic fluctuations in the upstream by the filamentation and/or Weibel type instabilities. The turbulence generated by the instabilities can alleviate Fermi-like diffusive process that accelerates X- and γ -ray emitting electrons. This is an important finding as it simultaneously addresses two problems – the termination shock formation in magnetized PWN winds and particle acceleration¹. Therefore, the combined action of the reconnection processes and shock acceleration is expected in the intense equatorial pulsar wind. Extensive PIC simulations in a wide dynamical range are needed to demonstrate the feasibility of this approach and identify the mechanism of particle acceleration to PeV energies and their synchrotron emission. However, to construct the synthetic spectra of the

Crab nebula at γ -ray energies (where the synchrotron cooling is very important), one needs to account for the radiative reaction force, which is not yet attainable in the PIC simulations (Sironi & Spitkovsky 2009; Nishikawa, et al. 2011).

Kinetic models can be used to simulate particle acceleration due to the repetitive interaction of electrons with magnetic turbulence in the energetic outflows with account for the synchrotron cooling. The kinetic model by Bykov & Meszaros (1996) for particle acceleration by both relativistic and transrelativistic shocks, accompanied by broad dynamic spectra of magnetic fluctuations with violent motions of relativistic plasma, predicts a hard broken power-law electron distributions with slopes $1 \leq p \leq 2$. In this model, particles are accelerated by strong magnetic fluctuations on timescales comparable to their gyration period in the r.m.s. magnetic field.

In the simulations described below we complement the kinetic model for particle acceleration in the vicinity of the striped wind termination shock with the synchrotron cooling effects to account for the spectral cut-off regime. To estimate the spectra of nonthermal leptons accelerated downstream of the PWN termination shock by Fermi mechanism, one can use a Fokker-Planck-type kinetic equation:

$$\frac{\partial N}{\partial t} = k(\gamma) \frac{\partial^2 N}{\partial z^2} - u \frac{\partial N}{\partial z} + \frac{1}{\gamma^2} \frac{\partial}{\partial \gamma} \gamma^2 \left[D(\gamma) \frac{\partial N}{\partial \gamma} + a(\gamma) N \right], \quad (1)$$

where z is the coordinate along the shock normal². This equation, averaged over the ensemble of strong electromagnetic fluctuations in the vicinity of the wind termination shock, accounts for diffusion and advection of electrons in phase space due to interactions with the fluctuations. The term with the momentum diffusion coefficient $D(\gamma)$ corresponds to the stochastic Fermi acceleration, $k(\gamma)$ is the fast particle spatial diffusion coefficient, u is the flow velocity component along the shock normal, and $a(\gamma)$ is the energy loss rate of an electron due to synchrotron radiation.

Model I. To construct the synchrotron emission spectra and flaring light curves in the diffusive shock acceleration model, we simulated spatially inhomogeneous accelerated pair distribution downstream of the termination shock of the striped wind using Eq. 1. Short-scale magnetic fluctuations are required to be present upstream of the shock to allow an efficient diffusive Fermi acceleration in the transverse relativistic shocks (see e.g. Bykov & Treumann 2011, and footnote ¹). Recently, Sironi & Spitkovsky (2011) have found in the PIC simulations that the fluctuations can be generated upstream of the *striped wind* termination shock. We assume the fluctuations provide the Bohm diffusion with $k(\gamma) \approx cr_g(\gamma)/3$. The stochastic Fermi acceleration was neglected in the model (i.e., $D = 0$).

To illustrate the intermittency effect in the cut-off regime, we simulated a light curve and spectra for a magnetic field fluctuation imposed in the GeV photon emitting region of scale size $\Delta_0 = 2 \times 10^{16}$ cm (for a quiescent magnetic field $B_0 = 0.2$ mG, downstream of the termination shock). The fluctuation $\delta B(t)$ is localized in a stripe of a $0.01\Delta_0$ width and has the time dependence shown by

¹ Note that the standard model of diffusive Fermi acceleration in a transverse relativistic shock in a non-striped uniform wind encounters problems when applied to PWN termination shocks, see, e.g., Niemiec et al. (2006); Pelletier et al. (2009); Bykov & Treumann (2011).

² Since the scale size Δ of the PeV electron distribution is much smaller than the termination shock radius, the problem can be considered as one-dimensional.

the solid line in Figure 1. Such magnetic field variations may be produced by the relativistic ion cyclotron instability at the termination shock. The instability, proposed by Spitkovsky & Arons (2004) to explain the origin of the optical wisps in the Crab nebula, can produce quasi-cyclic γ -ray flares in our model. The scale Δ_0 , used in our simulations, corresponds to about 0.1 of the magnetic field limit cycle found by Spitkovsky & Arons (2004) (see their Figure 2). The light curves of the γ -ray (0.5, 1 GeV and 2 GeV) and X-ray (5 keV) emission show the strong response of the γ -ray emission in the cut-off regime, while the response is very modest at X-ray energies. Note that the variability time in the GeV regime is shorter than the imposed field fluctuation and the cooling time of PeV electron distribution. This is because the emission in the cut-off regime is governed by high-order momenta of the magnetic field. The energy loss rate $a(\gamma)$ that determines the electron cooling depends on $\langle B^2 \rangle$. Therefore, the stochastic magnetic field realizations in the emission region with the same $\langle B^2 \rangle$ but different high-order momenta (determined by their PDFs) would correspond to the same particle distributions. However, their photon spectra in the cut-off regime are very different. This effect is clearly seen in Figure 3 discussed below. The synchrotron flares in the cut-off regime will appear even in the case of steady electron distributions.

In Figure 2 we show the simulated spectra of synchrotron emission, generated downstream of the termination shock, for $\eta \approx 0.5$, corresponding to quiescent regime (solid line) and fluctuation maximum (dashed line). They are similar to the quiescent and flare spectra observed in the Crab nebula by *AGILE* and *Fermi* (see Tavani et al. 2011; Abdo, et al. 2011; Vittorini et al 2011, and references therein).

Model II. Apart from the diffusive shock acceleration a variety of other particle acceleration mechanisms can be important in the region. The coalescence of magnetic islands, particle reflection by magnetic islands (both first and second order Fermi-type processes), are expected to be in action, as it occurs in the Earth magnetosphere (e.g. Drake et al. 2006; Zelenyi et al. 2010; Sironi & Spitkovsky 2011; Uzdensky et al. 2011; Daughton et al. 2011). When the source of strong turbulence is quasi-steady on timescales longer than $\omega_g^{-1}(\gamma)$, a simple analytical treatment of the problem is also possible. For the case of fast stochastic Fermi acceleration (comparable to the particle gyration period) by an energetic plasma outflow with strong magnetic turbulence, the momentum diffusion coefficient in Eq.1 takes the form $D(\gamma) = \gamma^2 \eta \omega_g(\gamma)$, where $\eta \lesssim 1$ is the particle acceleration time measured in the gyration times. Note that both $\omega_g(\gamma) = e \langle B^2 \rangle^{1/2} / (m_e c \gamma)$ and $a(\gamma) = 4r_0^2 \langle B^2 \rangle \gamma^2 / (9m_e c)$ (where $r_0 = e^2 / m_e c^2$) depend on the same ensemble-averaged value $\langle B^2 \rangle$.

The asymptotical shape of the particle spectrum in the cut-off regime is

$$N(\gamma) \propto \gamma^{-p} \exp \left[- \int d\gamma a(\gamma) / D(\gamma) \right]. \quad (2)$$

It is important that, while the index p depends on the turbulence spectrum and system geometry, the exponential cut-off in the particle spectrum is rather universal: $N(\gamma) \propto \gamma^{-p} \exp[-(\gamma/\gamma_0)^2]$, where $\gamma_0^2 = 9e\eta/(2r_0^2 \langle B^2 \rangle^{1/2})$, i.e., $\gamma_0 \approx 5 \times 10^9 \eta \langle B_{\text{mG}}^2 \rangle^{-1/4}$. The synchrotron emissivity

$\epsilon(\omega, B)$ in a local magnetic field B , which is assumed to be uniform on spatial scales larger than $r_f = m_e c^2 / eB$, is given by the equation

$$\epsilon(\omega, B, z) = \frac{\sqrt{3} B e^3}{2\pi m c^2} \int d\gamma \gamma^2 N(z, \gamma) R(\omega/\omega_c), \quad (3)$$

where $\omega_c = 3eB\gamma^2/2m_e c$ is the characteristic frequency of synchrotron radiation. Approximate analytic expressions for the function $R(x)$ were derived by Crusius & Schlickeiser (1986) and Zirakashvili & Aharonian (2007). The spectrum of synchrotron emission from the downstream region filled with strong magnetic field fluctuations can be expressed as

$$J(\omega) = \int dB dz \epsilon(\omega, B, z) P(B). \quad (4)$$

To illustrate the effect of the magnetic field fluctuations in the cut-off regime, where high-order statistical moments dominate the integral in Equation (4), we used the PDF of magnetosonic type fluctuations, which corresponds to the wisp structures seen in the polarized optical images presented by Hester (2008). The PDF has the form $P(B) = C_n \exp(-b^n/\Theta_n)$, with $n = 1$ and 2, and $b = |B - B_0|/B_0$. Here C_n is the normalization constant, and Θ_n is the dimensionless width of the distribution. The simulated synchrotron spectra are presented in Figure 3 for the gaussian ($n = 2$), exponential ($n = 1$), and non-fluctuating magnetic field distributions. The characteristic frequency ω_0 for the Lorentz factor γ_0 is given by $\hbar\omega_0 = 27\eta m_e c^2 / (4\alpha) \approx 470 \eta$ MeV. The synchrotron curves in Figure 3 are simulated for $\Theta_n = 1$ (i.e., for the case of strong fluctuations). The results illustrate a strong effect of the PDF shape on the spectral behaviour in the cut-off regime (even for a fixed rms field $\langle B^2 \rangle$), in contrast to a very modest effect in the power-law regime at $\omega < \omega_0$. Thus, Model II demonstrates that a reconstruction of the PDF tail of magnetic fluctuations in the synchrotron emission region (with the same $\langle B^2 \rangle$) would result in a strong change of the synchrotron photon spectrum, similar to that observed in the GeV flares in the Crab nebula.

3 DISCUSSION

In Model I, γ -ray photons are radiated downstream of the PWN termination shock by ultrarelativistic electrons. The particles are accelerated by some kind of Fermi mechanism in the vicinity of the termination shock in the striped wind with reconnecting magnetic fields. Electrons in the sharply decreasing high-energy tail of the distribution function radiate synchrotron γ -ray photons in fluctuating magnetic fields, which results in flaring behaviour in the cut-off regime (i.e., at the high-energy end of the synchrotron spectrum).

The compressed magnetic field structures, moving through the very narrow γ -ray emitting layer just downstream of the termination shock, result in γ -ray flares with the strong spectral variations shown in Figure 2. The timescale of the γ -ray photon variability in the flare is a fraction of the time $\Delta_0/c \sim 5 \times 10^5$ s in the cut-off regime because of the effect of high-order statistical moments. At the same time, the variability at energies below the cut-off energies is slower, and of much smaller amplitudes, as it is clearly seen from comparison of the light curves at

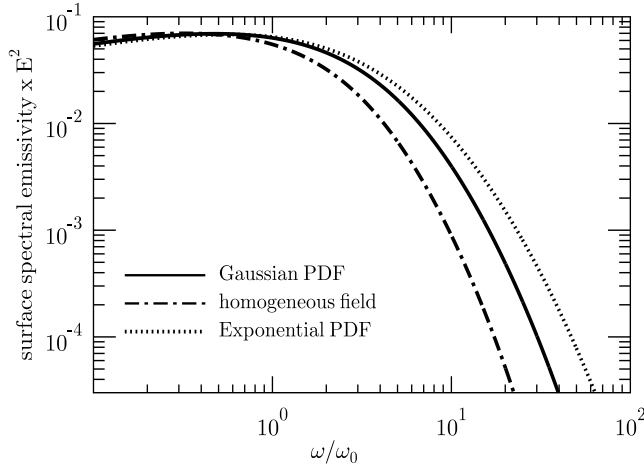


Figure 3. Surface spectral density of synchrotron radiation in the cut-off regime (in arbitrary units) simulated for different probability distribution functions of fluctuating magnetic field in the source (Model II). The characteristic frequency is defined by $\hbar\omega_0 \approx 470 \eta$ MeV.

5 keV and above 500 MeV in Figure 1. This is consistent with the lack of strong variations in the Crab at the X-ray and optical energies³ (Tennant et al. 2011; Caraveo et al. 2010). The frequency of the γ -ray flares is determined in our model by the frequency of occurrence of extreme values of magnetic fluctuations. The strong magnetic field compressions could be associated with the variable wisps observed with the quasi-periodic cycle of a year timescale (e.g. Scargle 1969; Hester et al. 2002; Bietenholz et al. 2004). To model the dynamics of the wisps, Spitkovsky & Arons (2004) simulated outward-propagating magnetosonic waves downstream of the shock generated by relativistic cyclotron instability of gyrating ions. The process achieves a limit cycle, in which the waves are launched with periodicity on the order of the ion Larmor time (a year timescale). Compressions in the magnetic field and pair density, associated with these waves, can reproduce the behaviour of the wisp and ring features. The high-resolution relativistic MHD models by Camus et al. (2009) have revealed a highly variable structure of the pulsar wind termination shock with quasi-periodic behaviour within the periods of about 2 years, and MHD turbulence on scales shorter than 1 year.

The synchrotron emission in the γ -ray regime is dominated by infrequent quasi-coherent structures, and therefore it should be highly polarized, that can be tested with future time resolved polarimetry observations.

The strong γ -ray variability predicted by our model is consistent with that observed in the Crab nebula. No simultaneous strong flares at other wavelengths is expected in our model. The γ -ray flares can occur even for a steady electron

distribution function with the maximal energies not exceeding the limit of particle acceleration by the Fermi mechanism with strong magnetic fluctuations at the extended wind termination shock. This is the main difference from the model by Yuan et al. (2011), which explains the flares by varying maximal electron energies in isolated knots that must transfer a substantial power (above 10^{36} erg s⁻¹) to the observed GeV photons. The variability of the maximal energies of the electrons would result in simultaneous GeV and 100 TeV regime flares since the electrons producing the synchrotron GeV photons radiate also 100 TeV regime photons by inverse Compton scattering. Also, Bednarek & Idec (2011) pointed out that the TeV photons produced by inverse Compton scattering of soft radiation by the variable distribution of accelerated electrons should be variable on timescales similar to those observed at GeV energies by *AGILE* and *Fermi-LAT*.

Recently, Komissarov & Lyutikov (2011) proposed a model in which the Crab flares originate in the inner knot (within about 1'' from the Crab pulsar) with strong Doppler beaming effects. In our model the region of GeV photon emission is about 10'' away from the pulsar. The Doppler-boosted synchrotron emission from a corrugated shock, proposed by Lyutikov et al. (2011), would be accompanied by flares in the cut-off regime of the inverse Compton TeV photons. This is different from the prediction of our model, in which the strong variability of GeV synchrotron emission is due to magnetic field variability, strongly amplified in the cut-off regime, while the amplitude of TeV emission variation is expected to be much less prominent.

We thank the referee J.Arons for constructive comments. A.M.B, G.G.P and Y.A.U were supported in part by the Russian government grant 11.G34.31.0001 to the Saint-Petersburg State Politechnical University, and also by the RAS Programs and by the RFBR grant 11-02-12082-ofi-m-2011. The numerical simulations were performed at JSCC RAS and the SC at Ioffe Institute. The research by A.M.B was supported in part by the National Science Foundation under Grant PHY05-51164 and by ISSI (Bern). G.G.P was supported in part by NASA grants NNX09AC84G and NNX09AC81G, and NSF grant AST09-08611.

REFERENCES

- Abdo A. A., et al. 2011, *Science*, 331, 739
- Arendt R. G., et al 2011, *ApJ*, 734, 54
- Arons J., 2008, in C Bassa, Z Wang, A Cumming and VM Kaspi ed., 40 years of pulsars: Millisecond Pulsars, Magnetars and More, AIP conf. proc. 983 Pulsars: Progress, Problems and Prospects. p. 200
- Arons J., 2011, in D. F. Torres & N. Rea ed., High-Energy Emission from Pulsars and their Systems A Tale of Two Current Sheets. pp 165
- Atoyan A. M., Aharonian F. A., 1996, *MNRAS*, 278, 525
- Bednarek W., Idec W., 2011, *MNRAS*, 414, 2229
- Bietenholz M. F., Hester J. J., Frail D. A., Bartel N., 2004, *ApJ*, 615, 794
- Bietenholz M. F., Kassim N., Frail D. A., Perley R. A., Erickson W. C., Hajian A. R., 1997, *ApJ*, 490, 291
- Bykov A. M., Ellison D. C., Renaud M., 2011, *Space Sci. Rev.*, pp 32

³ Note that we are discussing variations in the flux integrated over the downstream region (over z in our 1D model). The lack of strong variations in the flux does not contradict local variations in the synchrotron intensity, such as the moving wisps.

- Bykov A. M., Meszaros P., 1996, *ApJ*, 461, L37
- Bykov A. M., Treumann R. A., 2011, *Astron. Astroph. Rev.*, 19, 42
- Bykov A. M., Uvarov Y. A., Bloemen J. B. G. M., den Herder J. W., Kaastra J. S., 2009, *MNRAS*, 399, 1119
- Bykov A. M., Uvarov Y. A., Ellison D. C., 2008, *ApJ*, 689, L133
- Camus N. F., Komissarov S. S., Bucciantini N., Hughes P. A., 2009, *MNRAS*, 400, 1241
- Caraveo, P., et al. 2010, *The Astronomers Telegram*, 2903
- Crusius A., Schlickeiser R., 1986, *A&A*, 164, L16
- Daughton W., Roytershteyn V., Karimabadi H., Yin L., Albright B. J., Bergen B., Bowers K. J., 2011, *Nature Physics*, 7, 539
- de Jager O. C., Harding A. K., Michelson P. F., Nel H. I., Nolan P. L., Sreekumar P., Thompson D. J., 1996, *ApJ*, 457, 253
- Drake J. F., Swisdak M., Che H., Shay M. A., 2006, *Nat*, 443, 553
- Guilbert P. W., Fabian A. C., Rees M. J., 1983, *MNRAS*, 205, 593
- Hester J. J., 2008, *ARA&A*, 46, 127
- Hester J. J., Mori K., Burrows D., Gallagher J. S., Graham J. R., Halverson M., Kader A., Michel F. C., Scowen P., 2002, *ApJ*, 577, L49
- Kennel C. F., Coroniti F. V., 1984, *ApJ*, 283, 710
- Keshet U., Katz B., Spitkovsky A., Waxman E., 2009, *ApJ*, 693, L127
- Kirk J. G., Lyubarsky Y., Petri J., 2009, in W. Becker ed., *Astrophysics and Space Science Library Vol. 357, The Theory of Pulsar Winds and Nebulae*. pp 421
- Komissarov S. S., Lyutikov M., 2011, *MNRAS*, 414, 2017
- Lemoine M., Pelletier G., 2010, *MNRAS*, 402, 321
- Lyutikov M., Balsara D., Matthews C., 2011, *ArXiv e-prints*
- Niemiec J., Ostrowski M., Pohl M., 2006, *ApJ*, 650, 1020
- Nishikawa K., et al., 2011, *Advances in Space Research*, 47, 1434
- Pelletier G., Lemoine M., Marcowith A., 2009, *MNRAS*, 393, 587
- Rybicki G. B., Lightman A. P., 1979, *Radiative processes in astrophysics* Wiley-Interscience, New York
- Scargle J. D., 1969, *ApJ*, 156, 401
- Sironi L., Spitkovsky A., 2009, *ApJ*, 707, L92
- Sironi L., Spitkovsky A., 2011, *ApJ*, 741, 39
- Spitkovsky A., Arons J., 2004, *ApJ*, 603, 669
- Striani E. et al., 2011, *ApJ*, 741, L5
- Tavani M., et al., 2011, *Science*, 331, 736
- Tennant, A., et al. 2011, *The Astronomers Telegram*, 3283
- Uzdensky D. , Cerutti B., Begelman M. C., 2011, *ApJ*, 737, L40
- Vittorini V., et al 2011, *ApJ*, 732, L22
- Yuan Q., Yin P.-F., Wu X.-F., Bi X.-J., Liu S., Zhang B., 2011, *ApJ*, 730, L15
- Zelenyi L. M., Artemyev A. V., Malova K. V., Petrukovich A. A., Nakamura R., 2010, *Physics Uspekhi*, 53, 933
- Zimbardo G., Greco A., Sorriso-Valvo L., Perri S., Vörös Z., Aburjania G., Chargazia K., Alexandrova O., 2010, *Space Sci. Rev.*, 156, 89
- Zirakashvili V. N., Aharonian F., 2007, *A&A*, 465, 695